Onecut1 and Onecut2 redundantly regulate early retinal cell fates during development

Darshan Sapkota[a,b,c,d], Hemabindu Chintala[a,c,d], Fuguo Wu[a,c,d], Steven J. Fliesler[a,d,e], Zihua Hu[a,d,f,g,h], and Xiuqian Mu[a,b,c,d,i,1]

[a]Department of Ophthalmology/Ross Eye Institute, [b]Department of Biochemistry, [c]Developmental Genomics Group, [f]Department of Biostatistics, [g]Department of Medicine, and [h]Center of Computational Research, New York State Center of Excellence in Bioinformatics and Life Sciences, University at Buffalo, State University of New York, Buffalo, NY 14203; [d]State University of New York Eye Institute, Buffalo, NY 14203; [e]Research Service, Veterans Administration Western New York Healthcare System, Buffalo, NY 14215; and [i]Cancer Center Support Grant Cancer Genetics Program, Roswell Park Cancer Institute, Buffalo, NY 14263

Edited by Jeremy Nathans, The Johns Hopkins University, Baltimore, MD, and approved August 22, 2014 (received for review March 24, 2014)

Previously, we have shown that Onecut1 (Oc1) and Onecut2 (Oc2) are expressed in retinal progenitor cells, developing retinal ganglion cells (RGCs), and horizontal cells (HCs). However, in *Oc1*-null mice, we only observed an 80% reduction in HCs, but no defects in other cell types. We postulated that the lack of defects in other cell types in *Oc1*-null retinas was a result of redundancy with Oc2. To test this theory, we have generated *Oc2*-null mice and now show that their retinas also only have defects in HCs, with a 50% reduction in their numbers. However, when both *Oc1* and *Oc2* are knocked out, the retinas exhibit more profound defects in the development of all early retinal cell types, including completely failed genesis of HCs, compromised generation of cones, reduced production (by 30%) of RGCs, and absence of starburst amacrine cells. Cone subtype diversification and RGC subtype composition also were affected in the double-null retina. Using RNA-Seq expression profiling, we have identified downstream genes of Oc1 and Oc2, which not only confirms the redundancy between the two factors and renders a molecular explanation for the defects in the double-null retinas, but also shows that the onecut factors suppress the production of the late cell type, rods, indicating that the two factors contribute to the competence of retinal progenitor cells for the early retinal cell fates. Our results provide insight into how onecut factors regulate the creation of cellular diversity in the retina and, by extension, in the central nervous system in general.

transcription factors | neural development | retinal development | cell fate determination | gene regulation

The vertebrate retina is an essential part of the visual system, serving to receive light, transform that energy into electrical signals, and transmit them to the brain. The function of the retina is accomplished by an intricate and complex neural circuitry, which is composed of six major neuronal cell types wired up by stereotypic synaptic connections (1). During development, the retinal neurons and the only glial cell type, Müller glia, all arise from a common pool of retinal progenitor cells (RPCs) and the formation of each cell type is subject to precise and complex regulation (2). Gene regulation by transcription factors is the major mechanism by which differentiation of different retinal cell types is controlled and coordinated (3). Cell differentiation in the retina follows a distinct chronological order, with individual cells born at distinct, but overlapping, time windows (4). Based on the timing of their birth, the retinal cell types can be grouped into the early-born cell types, including retinal ganglion cells (RGCs), horizontal cells (HCs), cones, amacrine cells, and the late-born cell types, including rods, bipolar cells, and Müller cells.

In the mouse, genesis of the early-born cell types begins at around embryonic day (E) 11 and is largely completed at around birth of the animal, with peaks at around E14–15, whereas the late cell types are generated largely postnatally (4). It is believed that the competence in RPCs changes over time; thus RPCs at the early stages can only generate the early retinal cell types, and those from the late stages only give rise to the late cell types (2). Although many transcription factors regulating the individual retinal cell fates have been identified, how genesis of the different retinal cell types is coordinated remains poorly understood (3, 5). Regulators governing the transition of competence in RPCs from early stage to late stage are beginning to be identified. For example, deletion of the Lim-homeodomain gene *Lhx2* leads to prolonged production of the early retinal cell-type RGCs (6). Similarly, a group of microRNAs (let-7, miR-125, and miR-9) has also been shown to be required for this transition from the early phase to the late phase (7). However, it is not clear what defines the early and late competence and whether shared mechanisms coordinate the births of all of the early or late cell fates.

The members of the "onecut" family of transcription factors play diverse developmental roles (8–12). In the mouse, three onecut factors, Onecut1 (Oc1), Onecut2 (Oc2), and Onecut3 (Oc3), with essentially identical DNA-binding domains exist (13). All three of these factors are expressed in the mouse retina, with Oc1 and Oc2 being at high levels (14, 15). Oc1 and Oc2 have overlapping expression patterns in RPCs at early developmental stages as well as in precursors of RGCs, cones, and HCs throughout development (15). The temporal and spatial patterns of Oc1 and Oc2 expression indicate that they likely function in the early retinal cell types. Nevertheless, in *Oc1*-null retinas, only HCs are affected, with an 80% reduction in their numbers (14). This result may be caused by redundancy between Oc1 and Oc2, because they have highly overlapping expression patterns and high degree of identity in their DNA-binding domains. To further investigate the roles onecut

Significance

We show that the onecut transcription factors, Onecut1 and Onecut2, redundantly regulate the formation of all four early-born retinal cell types, namely horizontal cells, ganglion cells, cones, and amacrine cells, and prevent precocious formation of the late retinal cell type, rods. Expression profiling suggests these two factors regulate a shared set of downstream genes to maintain competence for the early retinal cell types and to regulate generation of various subtypes of retinal ganglion cells. This study lays the foundation for further examination of how onecut factors regulate cell differentiation in the retina, as well as in the central nervous system in general.

Author contributions: D.S. and X.M. designed research; D.S., H.C., F.W., and S.J.F. performed research; D.S., S.J.F., Z.H., and X.M. analyzed data; and D.S. and X.M. wrote the paper.

The authors declare no conflict of interest.

This article is a PNAS Direct Submission.

Data deposition: The sequences reported in this paper have been deposited in the National Center for Biotechnology Information Sequence Read Archive, www.ncbi.nlm.nih.gov/sra (accession nos. SAMN02688949–SAMN02688960).

[1]To whom correspondence should be addressed. Email: xmu@buffalo.edu.

This article contains supporting information online at www.pnas.org/lookup/suppl/doi:10.1073/pnas.1405354111/-/DCSupplemental.

factors play in retinal development, we generated a floxed *Oc2* allele and deleted it specifically in the developing retina by the retina-specific *Six3-cre* mouse line (14). Similar to the *Oc1* knockout, but to a lesser degree, deletion of *Oc2* resulted in only the loss of HCs by about 50%. In contrast, *Oc1*/*Oc2* double knockout (DKO) retinas had more severe defects, including a complete loss of HCs as well as compromised development of cones, RGCs, and starburst amacrine cells (SACs), indicating that Oc1 and Oc2 indeed function redundantly in the early retinal cell types. We also performed retinal transcriptome profiling by RNA-Seq and identified genes whose expression changed because of deletion of Oc1 and Oc2. The known functions of some of these genes further indicate that Oc1 and Oc2 are essential not only for promoting the early retinal cell fates, but also for prohibiting the late cell fates (e.g., rods).

Results

Defects in *Oc2*-Null Retinas. We first generated a floxed *Oc2* allele ($Oc2^{flox}$) by inserting loxP sites into regions flanking the first exon, which encodes the cut domain and a part of the homeo domain (Fig. S1 *A* and *B*). Retina-specific inactivation of *Oc2* was achieved by crossing $Oc2^{flox}$ mice with the *Six3-Cre* mice (Fig. S1 *C* and *D*). The $Oc2^{flox/fox}$;*Six3-Cre* mice expressed essentially no Oc2 (Fig. S1*D*) and will be referred to as *Oc2*-null hereafter. Histological analysis (H&E staining) of mature retinal sections indicated that *Oc2*-null retinas were well laminated, and all of the retinal layers were comparable to those of the control (wild-type) retinas (Fig. S1 *E* and *F*). Occasionally the outer plexiform layer (OPL) was disrupted by retinal cells (Fig. S1*F*), which may be a result of defects in HCs (see below). We next examined whether deletion of *Oc2* affected any retinal cell types: we performed immunofluorescence analysis of postnatal day (P) 25 retinal sections, using antibodies against a variety of cell-type–specific markers (Fig. S2 *A*–*P*). Most cell types, including cones, rods, bipolar cells, Müller glial cells, RGCs, and amacrine cells, did not show any change in their numbers, relative to the controls, as confirmed by cell counting (Fig. S2*Q*). However, similar to what was observed in *Oc1*-null retinas, there was a marked reduction of HCs in *Oc2*-null retinas, as demonstrated by immunofluorescence staining of NF160 on retinal sections, although RGCs that also express this marker did not change (Fig. S2 *O* and *P*). To obtain a more accurate count of the loss of HCs, we performed flat-mount immunofluorescence staining for calbindin and observed a 47% loss in *Oc2*-null retinas, relative to the controls (Fig. 1 *A*, *B*, and *E*). To ascertain when the loss of HCs occurred, we also examined *Oc2*-null retinas with the early HC marker Prox1 at E14.5, and found a 46% reduction in the number of HCs (Fig. 1 *C*, *D*, and *F*). These results demonstrate that *Oc2*-null retinas have a very similar, but less severe, phenotype compared with *Oc1*-null retinas (14), and that the loss of HCs is a result of reduced genesis during retinal development.

Complete Failure of HC Formation and OPL Development in *Oc1*/*Oc2* DKO Retinas. The relatively moderate defects in both *Oc1*- and *Oc2*-null retinas, despite the much broader expression patterns of Oc1 and Oc2, suggested that the two factors function redundantly to regulate retinal development. To test this possibility, we generated *Oc1*/*Oc2* double-knockout mice ($Oc1^{flox/flox}$;$Oc2^{flox/flox}$;*Six3-Cre*, referred to as DKO hereafter). We first characterized the development of the DKO retina by histological analysis. As shown in Fig. 2, the mature DKO retina was well-laminated with most histological retinal layers, but was clearly abnormal compared with the wild-type control retina (Fig. 2 *A* and *B*). The most obvious defect was the complete absence of the OPL, resulting in the fusion of the outer nuclear layer (ONL) and inner nuclear layer (INL). The INL and inner plexiform layer (IPL) of DKO retinas were also slightly thinner than those of wild-type retinas. The complete collapse of the OPL indicated a severe loss of HCs. This finding was confirmed by immunofluorescence labeling of mature (P25) DKO

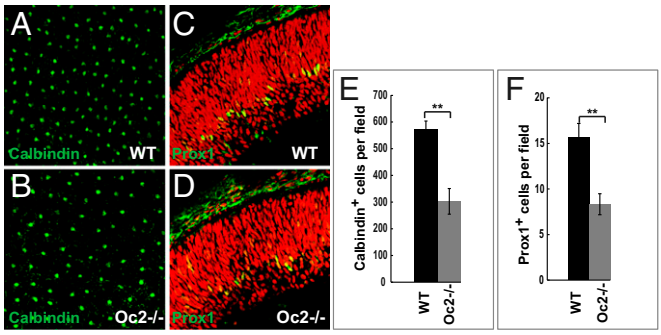

Fig. 1. Partial loss of HCs in the *Oc2*-null retina. (*A* and *B*) P25 retinal whole mounts stained for calbindin to label mature HCs in wild-type (WT) and *Oc2*-null ($Oc2^{-/-}$) retinas. (*C* and *D*) E14.5 wild-type and *Oc2*-null retinal sections stained with anti-Prox1 (green) to label developing HCs. Red is propidium iodide staining. (Magnification: *A*–*D*, 200×.) (*E*) Counting of calbindin$^+$ cells in *A* and *B*. (*F*) Counting of Prox1$^+$ HC precursors in *C* and *D*. For both *E* and *F*, positive cell counts were from the corresponding regions of wild-type and mutant retinas. Error bars indicate ± SD. $n = 3$, $^{**}P \leq 0.01$.

retinas for HC markers, including calbindin, NF160, and Lim1 (Fig. 2 *C*–*H*). Expression of all these markers was completely absent at the location typical for HCs in the DKO retinas (Fig. 2 *D*, *F*, and *H*), although the expression of NF160 and calbindin in other cell types was still detected (Fig. 2 *D* and *F*), implying that the cell loss was HC-specific. To check whether this was a developmental defect, as is the case in the single knockouts, we examined HC formation in the DKO retina at E14.5. Whereas the two early HC markers, Lim1 and Prox1, were readily detected in wild-type retinas (Fig. 2 *I* and *K*), no Lim1$^+$ or Prox1$^+$ cells were detected in DKO retinas at this stage (Fig. 2 *J* and *L*). Thus, HC development was totally abolished in the absence of Oc1 and Oc2. Because HC genesis is only partially diminished in Oc1 and Oc2 single-null mice, the complete failure of HC genesis in the DKO mouse was consistent with our hypothesis that these two factors act redundantly to regulate the HC fate.

The collapse of the OPL in the DKO retinas was consistent with previous findings that development of the OPL is dependent on HCs (14, 16). Loss of HCs leads to loss of ribbon synapses and flat contacts between photoreceptors and bipolar cells (14, 16). To further characterize the defects in the OPL in the DKO retina, we used fluor-conjugated peanut agglutinin (PNA) to stain the cone flat contacts with bipolar cells. Whereas these contacts were readily observed in the wild-type retina, they were essentially absent in the DKO retina (Fig. 2 *M* and *N*). The synaptic ribbons mark the position of the triad synapses formed between photoreceptors, HCs, and bipolar cells, whereas processes from bipolar cells make synaptic connections with photoreceptors and stop at the inner third of the OPL. This fact was clearly demonstrated by the costaining of synaptic ribbons with anti-Bassoon and rod bipolar cells with anti-Pkcα in wild-type retinas (Fig. 2*O*). In the DKO retina, however, the synaptic ribbons were almost completely diminished (Fig. 2*P*), and the processes from the rod-bipolar cells extended all of the way into the ONL (Fig. 2*P*). In addition, the soma of some bipolar cells could be observed in the ONL (Fig. 2*P*). These results indicate that HCs are essential for the development of synaptic connections in the OPL, and thereby its formation and the normal lamination of the ONL and INL.

Onecut Factors Are Required for Cone Photoreceptor Development. At E14.5, the mouse retina contains Oc1-expressing RPCs in the outermost ventricular zone, which overlap with early cone makers, suggesting a role for Oc1 in cone genesis (15, 17). However, *Oc1*-null retinas did not show any change in the cone population except for reduction in the numbers of cone pedicles (14), likely a secondary effect from the loss of HCs and the subsequent defective

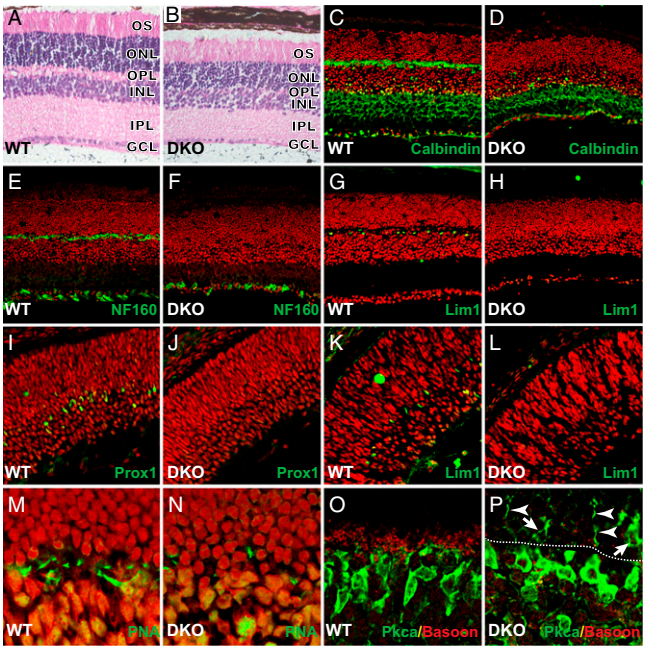

Fig. 2. Loss of HCs in *Oc1*/*Oc2* DKO retinas. (*A* and *B*) H&E staining of mature wild-type and DKO retinal sections. Note the complete collapse of the ONL in the mature DKO retinas (*B*). (*C*–*H*) Immunofluorescence staining for the HC markers calbindin (*C* and *D*), NF160 (*E* and *F*), Lim1 (*G* and *H*) in sections from mature (P25) wild-type and DKO retinas. (*I*–*L*) Immunofluorescence staining for Prox1 and Lim1 on E14.5 wild-type and DKO sections. (*M*–*P*) Immunofluorescence labeling for cone pedicles with PNA (*M* and *N*), synaptic ribbons with anti-Bassoon and rod bipolar cells with anti-Pkcα (*O* and *P*) in WT and DKO retinal sections at P25. (Magnification: *A*–*L*, 200×; *M*–*P*, 400×.) OS, outer segment layer. Red in panels *C*–*L* is propidium iodide staining. In *P*, dotted line demarcates the ONL and INL in the DKO retina, arrowheads indicate ectopic sprouting of bipolar processes into the OPL, and arrows point to ectopically positioned somas of bipolar cells in the ONL.

development of the OPL. We also did not observe obvious defects in cones in *Oc2*-null retinas (Fig. S2 *A*–*D*). On the other hand, a recent study suggested that Oc1 promotes the cone fate by regulating expression of the cone precursor genes thyroid hormone receptor beta (Thrb) and retinoid x receptor gamma (Rxrγ) (17). To clarify this issue, we examined the development of cones in both single- and double-knockout retinas at E14.5, a time when cone production begins to peak, using immunofluorescence staining for Rxrγ. Consistent with what was observed in mature retinas, the numbers of cone precursors in *Oc1*- and *Oc2*-null retinas were comparable to those in the wild-type control retina (Fig. S3 *A*–*C*). However, in DKO retinas essentially no Rxrγ expression was observed in the apical side of the retina at E14.5, although its expression in RGCs was unaffected compared with the wild-type retina (Fig. 3 *A*, *B*, and *U*). At E17.5, some cone precursors began to appear (Fig. 3 *C*, *D*, and *U*). By P5, there were about 34% fewer cones detected in DKO retinas, compared with wild-type ones (Fig. 3 *E*, *F*, and *U*). A similar (30%) loss of cones persisted through adulthood (Fig. 3 *G*, *H*, and *U*), which was further confirmed by immunostaining of two other cone markers, cone arrestin (CAR) and PNA (Fig. S3 *D*–*G*). In addition, we observed that the staining for the cone pedicles was severely diminished (Fig. S3 *E* and *G*), indicating that the morphology of cones was also altered. This defect likely resulted from abnormal OPL formation, as similar but less-severe phenotypes also were observed in the single-knockout retinas, where the cone numbers did not change (Fig. S2*D*) (15).

Next, we examined how the two cone subtypes were affected in the DKO retina, using whole-mount immunolabeling of S- and M-cones with anti–S-opsin and anti–M-opsin, respectively (Fig. 3 *I*–*T*). In the wild-type retina, S- and M-cones are distributed in two opposing gradients: the densities of S-cones are high on the ventral side and low on the dorsal side (Fig. 3 *I*–*K*), whereas the densities of M-cones are high on the dorsal side and low on the ventral side (Fig. 3 *O*–*Q*) (18). Thus, normally ∼55% of cones in the ventral side are S-cones and ∼95% of cones in the dorsal side are M-cones (Fig. 3 *V* and *W*). However, in the DKO retina the distribution gradients were disrupted for both S- and M-cones (Fig. 3 *L*–*N* and *R*–*T*). The densities of S-cones on the dorsal and ventral sides were almost equivalent (Fig. 3 *M*, *N*, and *V*), with S-cones accounting for ∼90% of cones on both sides. Although the dorsal/ventral gradient of M-cones could still be observed, their densities were significantly decreased (Fig. 3 *S* and *T*), with M-cones accounting for only about 10% of all cones on both sides (Fig. 3*W*). Therefore, apart from reduced production, cones also exhibited a failure to diversify into the M-subtype in the DKO retina.

DKO of *Oc1* and *Oc2* Leads to Defects in RGCs. The lack of RGC defects in the *Oc1*- and *Oc2*-null retinas likely was also because of the redundancy of the two transcription factors. To test this idea, we first examined whether there were any changes in the optic nerves of the DKO mouse. The DKO optic nerve was markedly thinner than that of the wild-type retina (Fig. 4*A*), which was further confirmed by cross-sectioning of the optic nerves (Fig. 4 *B* and *C*). Furthermore, by transmission electron microscopy on cross sections, we observed that the optic nerve axons from DKO mice were hypomyelinated at P16, compared with those from wild-type mice (Fig. 4 *D* and *E*). At P30, when myelination of the optic nerve is almost complete in the wild-type mouse, most RGC axons also were myelinated in the DKO optic nerves (Fig. 4 *F* and *G*). However, the g-ratios (i.e., the ratio of the inner axonal diameter to the total diameter), which often is used as a measure of axon myelination, were significantly greater for DKO optic nerves than for wild-type optic nerves (Fig. 4*H*), indicating that the DKO axons remained hypomyelinated. In addition, there also was a significant loss of large caliber (>1-μm diameter) axons in the DKO optic nerve, as demonstrated by comparing the distribution of axonal diameters in wild-type vs. DKO optic nerves (Fig. 4*I*). All of these observations indicated that RGCs in the DKO retina were defective. We next performed flat-mount immunostaining for the RGC markers phosphorylated neurofilament heavy chain (SMI32), Pou4f1, and Pou4f2. Consistent with the thinner optic nerve, staining for SMI32 revealed that the optic fibers in DKO retinas were much thinner, compared with those from wild-type retinas, although these fibers were well fasciculated and projected to the optic disk normally (Fig. 4 *J* and *K*). Both Pou4f1 and Pou4f2 are expressed in a large percentage of RGCs (19). Consistent with the thinning of optic fibers, the numbers of Pou4f1$^+$ and Pou4f2$^+$ cells were both reduced by ∼30% (Fig. 4 *L*–*P*). Therefore, in contrast to *Oc1*- and *Oc2*-null retinas, there was a significant reduction in the number of RGCs in the DKO retina.

We further attempted to understand when the loss of RGCs occurred during development, using immunofluorescence staining for the early RGC markers Isl1 at different developmental stages (Fig. 5 *A*–*H*). At E14.5, we observed no obvious difference in Isl1$^+$ cells between DKO and wild-type retinas in the developing ganglion cell layer (GCL) (Fig. 5 *A*, *B*, and *I*). Nevertheless, even at this early stage, there was a significant reduction in newly forming RGCs located in the outer neuroblast layer (ONBL) (Fig. 5 *B* and *I*). By E17.5, however, the numbers of RGCs were significantly less in the DKO retina than in the wild-type retina, and newly forming RGCs in the ONBL continued to be decreased in number (Fig. 5 *C*, *D*, and *I*). This decrement in RGCs persisted at later stages, such as P0 (Fig. 5 *E*, *F*, and *I*) and P25 (Fig. 5 *G*, *H*, and *I*). Examination of another early RGC marker, Pou4f2, revealed similar results (Fig. S4). In sum, these data suggest that reduced RGC formation occurred at relatively

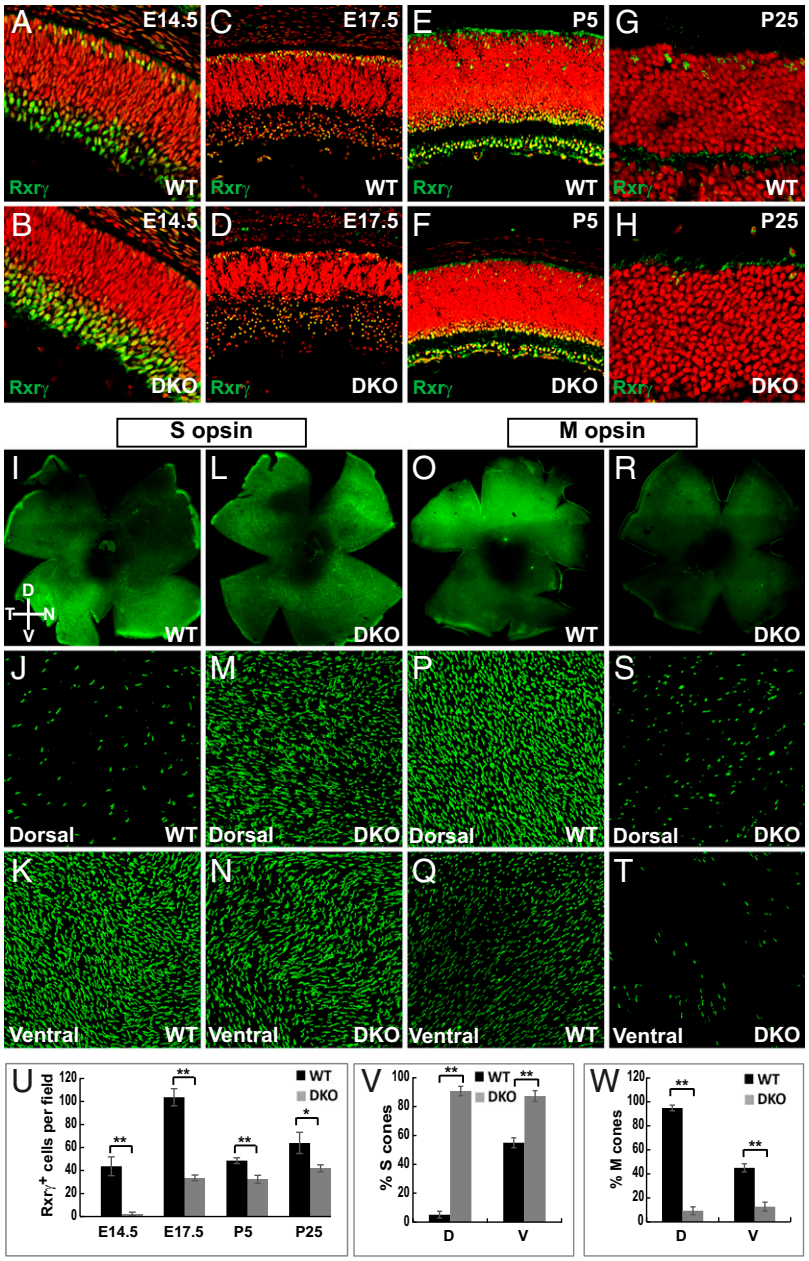

Fig. 3. Defect in the genesis and subtype diversification of cones in *Oc1/Oc2* DKO retinas. (*A–H*) Cone development analyzed by immunostaining of wild-type and DKO retinal sections with anti-Rxrγ at E14.5 (*A* and *B*), E17.5 (*C* and *D*), P5 (*E* and *F*), and P25 (*G* and *H*). (*I–T*) Cone subtypes immunolabeled on P25 whole retinas using anti–S-opsin (*I–N*) and anti–M-opsin (*O–T*). (Magnification: *A–H*, *J*, *K*, *M*, *N*, *P*, *Q*, *S*, and *T*, 200×; *I*, *L*, *O*, and *R*, 50×.) (*U*) Quantitation of cones in *A–H*. (*V* and *W*) Quantitative analysis of distribution of S-cones in *I–N* (*V*) and M-cones in *O–T* (*W*). Cell counts from the corresponding regions of wild-type and DKO were plotted as mean ± SD, and Student's *t* test was applied to determine statistical significance. $n = 3$, $^{*}P \leq 0.05$, $^{**}P \leq 0.01$. Red in panels *A–H* is propidium iodide staining. In ***I***, D, dorsal; N, nasal; T, temporal; V, ventral.

late stages, beginning at around E14.5, and that this reduced RGC genesis was likely responsible for the reduced RGC numbers seen in later stages.

The observation of only an ∼30% reduction in the numbers of RGCs in DKO retinas prompted us to investigate whether only certain RGC subpopulations required the onecut factors for development. We first examined the expression of Tbr2 (also known as Eomes) through the different stages of retinal development (Fig. 6 *A–H*). Tbr2 is expressed in only a subset of RGCs (20), some of which eventually become intrinsically photosensitive RGCs (ipRGCs) (21). At E14.5, we observed a near complete loss of Tbr2 expression in DKO retinas, compared with wild-type retinas in which a subset of RGCs were Tbr2^{+} (Fig. 6 *A*, *B*, and *M*). At E17.5, there were only occasional Tbr2^{+} RGCs in DKO retinas, whereas expression was maintained in the subset of RGCs in wild-type retinas (Fig. 6 *C*, *D*, and *M*). At later stages (P0 and P25), the numbers of Tbr2^{+} RGCs in DKO retinas were about 53% of those found in wild-type retinas (Fig. 6 *E–H* and *M*). Consistent with the roles of Tbr2 in ipRGCs (21), we also observed a 50% loss of intrinsic ipRGCs in the DKO retina as detected by immunofluorescence staining for melanopsin (Fig. 6 *I*, *J*, and *N*). In contrast, another RGC subtype, the On-Off direction-selective RGCs (dsRGCs), labeled by anti-CART (cocaine- and amphetamine-regulated transcript) staining (22), exhibited only a 33% loss,

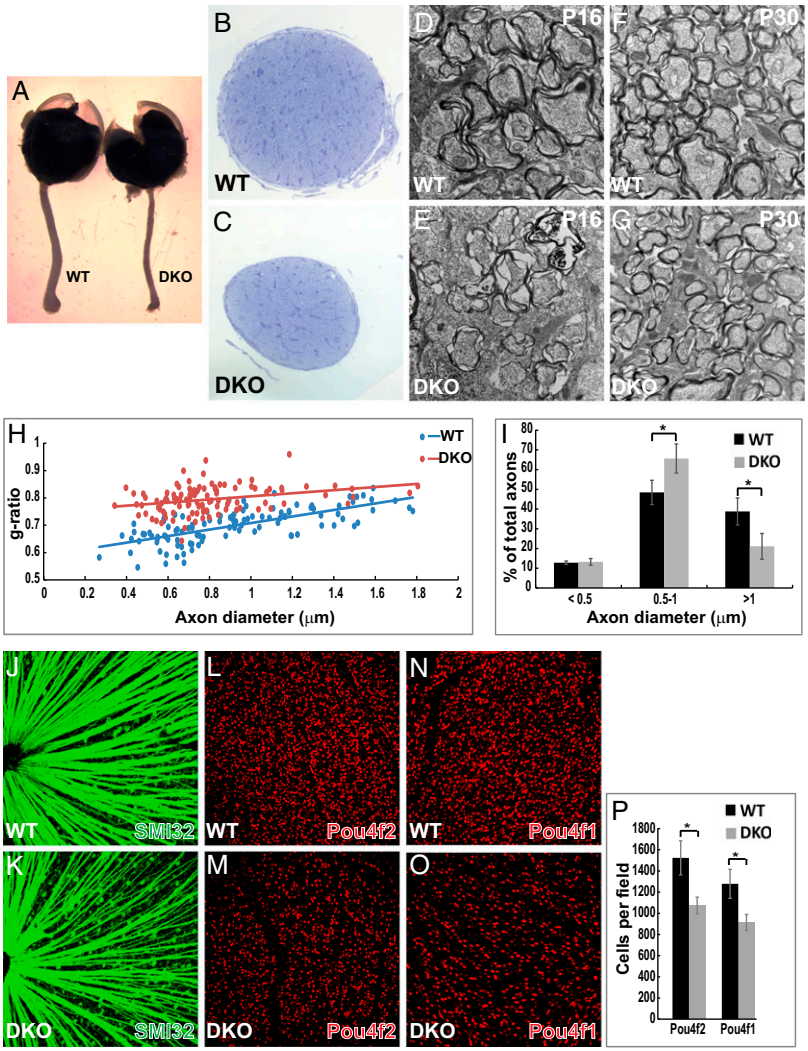

Fig. 4. Loss of RGCs in *Oc1/Oc2* DKO retinas. (*A–C*) Examination of whole eyes (*A*) and histological cross-sections of optic nerves (*B* and *C*) reveals thinning of the optic nerve in the DKO mouse compared with that in the wild-type mouse. (*D–G*) Representative electron micrographs of optic nerve sections at P16 (*D* and *E*) and P30 (*F* and *G*) from wild-type and DKO mice. (*H*) A scatterplot showing g-ratios of myelinated axons as a function of the corresponding inner axon diameter in P25 optic nerves from wild-type and DKO mice. (*I*) Distribution of axons with different ranges of axonal diameters in wild-type and DKO optic nerves. (*J* and *K*) Whole retinas (P25) labeled with SMI32 showed fewer and thinner optic fibers in the DKO retina. (*L–O*) Whole retinas from wild-type and DKO mice (P25) stained for RGC markers Pou4f2 (*L* and *M*) and Pou4f1 (*N* and *O*). (Magnification: *B* and *C*, 100×; *D–G*, 5,000×; *J–O*, 200×.) (*P*) Quantification of cells in *L–O*. Cell counts were plotted as mean ± SD, and Student *t* test was applied to determine statistical significance. $n = 3$, $^*P \leq 0.05$.

which was similar to the extent of total RGC loss (Fig. 6 *K*, *L*, and *O*). These results indicate that certain RGC subtypes were more severely affected by the deletion of *Oc1/Oc2*.

Defects in Other Retinal Cell Types in DKO Mice. We also examined how other retinal cell types—namely rods, bipolar cells, Müller glial cells, and amacrine cells—were affected in DKO mice. As determined by immunostaining for rhodopsin, the rods in DKO retinas were grossly normal, both in numbers and morphology (Fig. S5 *A*, *B*, and *M*). Bipolar cells, as detected by anti-Chx10 immunostaining (Fig. S5 *C* and *D*), showed a slight reduction (16%) in their numbers in DKO retinas compared with controls (Fig. S5*M*). Staining with anti-vimentin and anti-Sox9 revealed no obvious changes in the numbers of Müller glial cells (Fig. S5 *E–H* and *M*). However, Müller glial cell processes in the OPL of DKO retinas were greatly reduced in number (Fig. S5*F*), which might be a consequence of the defective development of the OPL (see above). The positions of the somas of Müller cells also appeared abnormal (Fig. S5*H*). Instead of being located at the center of the INL, as in wild-type retinas, the Müller cell somas in DKO retinas were located closer to the upper boundary of the INL, and were more disorganized compared with those in wild-type retinas. The numbers of amacrine cells, as detected by anti-syntaxin I and anti-Pax6 immunostaining, were reduced by 32% in the DKO retina compared with the wild-type retina (Fig. S5 *I–L* and *M*). Isl1 is also a marker for SACs, which are located in the GCL and the inner side of the INL (23) (Fig. 5 *E* and *G*). Interestingly, in DKO retinas, few Isl1-expressing SACs in the INL could be detected (Fig. 5 *F* and *H*). We further confirmed this with another SAC marker, choline acetyltransferase (ChAT), by flat-mount immunofluorescence staining. In wild-type retinas, the SACs could be readily observed in both the GCL and the inner side of the INL (Fig. 7 *A* and *C*). In DKO retinas, however, very few, if any, $ChAT^+$ SACs were detected in either the GCL or the INL (Fig. 7 *B* and *D*). These results indicate that SACs were more severely affected than the general amacrine cell population. Because Oc1 and Oc2 are not expressed in bipolar or amacrine cells, it is likely that the observed reduction of these cell types was an

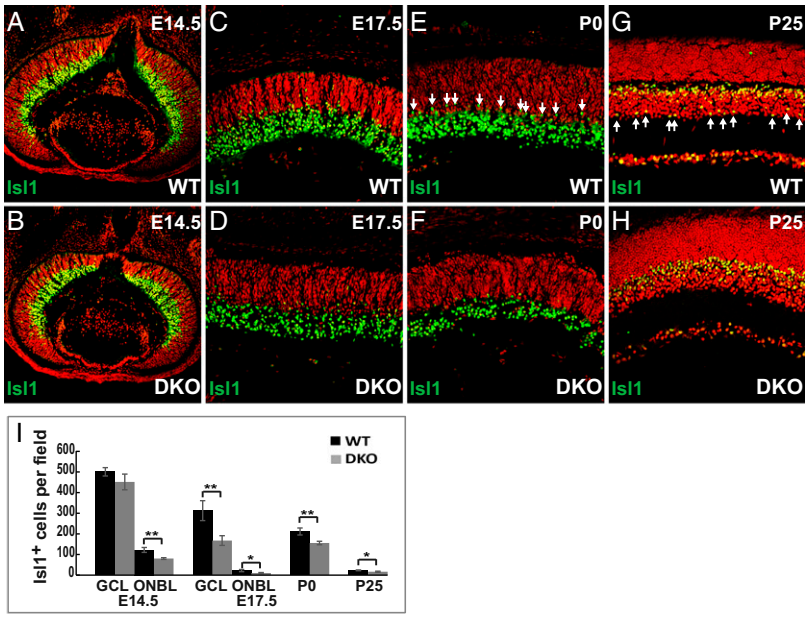

Fig. 5. Reduced generation of RGCs in *Oc1*/*Oc2* DKO retinas during development. (*A*–*H*). RGC genesis analyzed by immunolabeling of wild-type and DKO retinal sections with anti-Isl1 (green) at indicated stages. Red is propidium iodide staining. Reduced development of RGCs is seen as early as E14.5 in the ONBL of the DKO retina (*B*). Note the presumptive SACs labeled by Isl1 (arrows in *E* and *G*), which are lost in the DKO retina (*F* and *H*). (Magnification: *A* and *B*, 100×; *C*–*H* 200×.) (*I*) Quantitative analysis of Isl1$^+$ RGCs at different stages. Student *t* test was applied to determine statistical significance. Error bars indicate ± SD. $n = 3$, $^*P \leq 0.05$, $^{**}P \leq 0.01$.

indirect effect; however, this needs to be confirmed unequivocally by lineage-tracing experiments. We also do not know how the onecut factors are involved in SAC development, because currently there are no suitable markers to study their genesis during early developmental stages.

Changes in Apoptosis, Cell Proliferation, and Global Gene Expression in DKO Retinas. We performed pulse 5-ethynyl-2′-deoxyuridine (EDU) labeling and TUNEL assays to investigate whether or not there were any changes in cell proliferation or apoptosis, respectively, in DKO retinas. By EDU labeling, we did not see significant differences in the numbers of proliferating progenitor cells between the DKO and the wild-type retinas at E14.5 (Fig. S6 *A*, *B*, and *Q*). At E17.5, however, there was about 25% reduction in the number of EDU$^+$ progenitors in DKO retinas, compared with wild-type retinas (Fig. S6 *C*, *D*, and *Q*). Because the reduced proliferation happens later than the peaks of cone, HC and RGC generation, it may not have contributed significantly to the loss of these cell types, although it may have resulted in the reduction of the late-born cell types, such as bipolar cells. As to apoptosis, we did not find significant differences in the number of TUNEL$^+$ cells in DKO retinas compared with wild-type retinas from E14.5 to P5 (Fig. S6 *E*–*L* and *R*). However, at P16 and P25, there was a marked increase in the number of TUNEL$^+$ cells in DKO retinas, relative to controls, but these cells were largely confined to the photoreceptor layer (Fig. S6 *M*–*P* and *R*), which was likely secondary to the loss of HCs, as is the case in the *Oc1*-null retina (15). Therefore, apoptosis did not contribute to the reduced number of HCs, cones, or RGCs in the DKO retina.

To gain further insight into how these two factors regulate retinal development, we performed RNA-Seq analysis for wild-type, *Oc1*-null, *Oc2*-null, and DKO retinas at E14.5. We identified 163 genes in DKO, 85 genes in *Oc1*-null, and 31 genes in *Oc2*-null retinas, with altered expression levels (Fig. 8 *A* and *B* and Dataset S1). The finding that DKO retinas had the largest, *Oc1*-null retinas had an intermediate, and *Oc2*-null retinas had the smallest number of genes altered in expression was consistent with the relative severities of the retinal phenotypes in the three genotypes. In addition, most genes affected in *Oc1*-null (62 of 85) and *Oc2*-null (27 of 31) retinas were found in the DKO gene list (Fig. 8*B*). The *Oc1*-null and *Oc2*-null lists also exhibited considerable overlap with each other. More importantly, the vast majority of genes demonstrated the same trend of changes in all three mutants. In other words, although far more genes showed significant changes in DKO retinas compared with the *Oc1*- or *Oc2*-null retinas, these genes tended to have the same direction of changes in the single-knockouts as in the DKO, only to a lesser degree. This was clearly demonstrated by the heat map (Fig. 8*A*), in which most genes presented the same color across the three mutants. These results not only indicate that Oc1 and Oc2 largely regulate the same set of downstream genes, but also provide a molecular interpretation for the redundancy of Oc1 and Oc2 in retinal development.

Furthermore, the identities of many of the genes downstream of the onecut factors suggest the complex roles they play in the developing retina. Many of these were transcription factor genes known to regulate retinal cell fates, and the rest were known to encode proteins specific to retinal cell types (Fig. 8*C* and Dataset S1). We confirmed the changes of some of these genes in the DKO retina by quantitative PCR (Fig. S7). Consistent with the observed phenotypes, we found a significant down-regulation of genes known to regulate the differentiation of cones (Thrb and Rxrγ) or HCs (Prox1) (Fig. 8*C*). Interestingly, we observed bidirectional changes of genes expressed in RGCs. Whereas some RGC genes, including *Pou6f2*, *Irx6*, *Irx5*, *Irx3*, and *Crabp1*, displayed significant down-regulation in the DKO retina, other RGC genes, such as *Gfi1*, *Isl2*, and *Igf1*, were markedly up-regulated (Fig. 8*C* and Dataset S1). However, many other RGC markers, including *Isl1* and *Pou4f2*, did not show any appreciable changes in DKO retinas. Many of the RGC genes affected in the DKO retina, including *Pou6f2*, *Crabp1*, *Gfi1*, and *Isl2*, are expressed only in subsets of RGCs (24–28) (Fig. 8 *D*, *F*, *H*, and *J*). Although these subsets of RGCs have not been well characterized, at the molecular level they can be considered RGC subtypes. In fact Isl2$^+$ cells have been shown to represent distinct RGC subtypes, including most α-RGCs (26). By in situ hybridization, we further

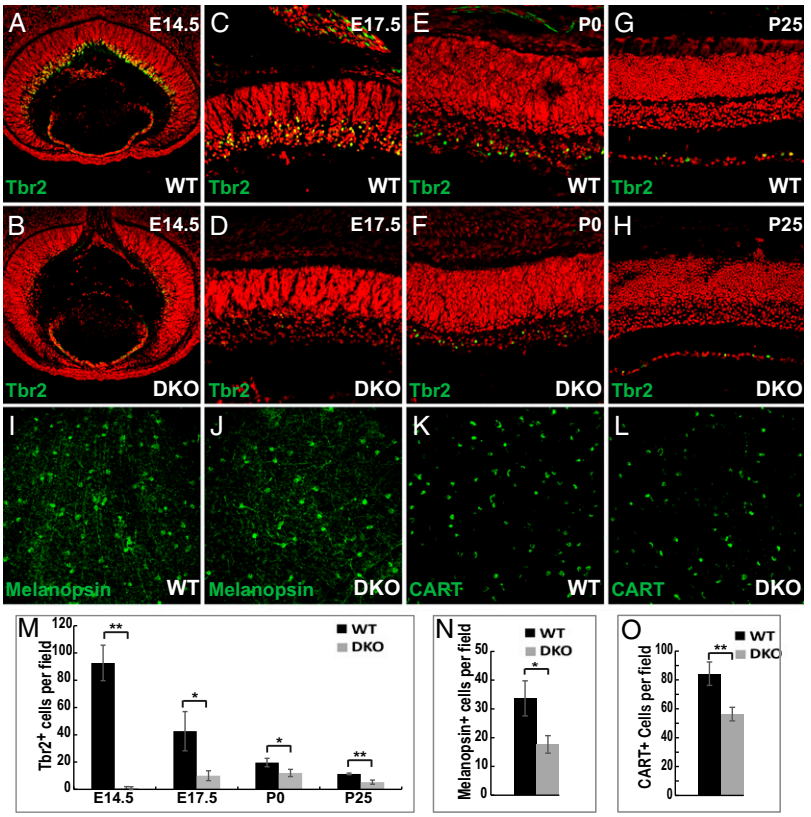

Fig. 6. RGC subtypes in Oc1/Oc2 DKO retinas. (*A–H*) Immunostaining for Tbr2 (green) in wild-type and DKO retinal sections of indicated ages. Red is propidium iodide staining. (*I–L*) Flat-mount immunostaining for melanopsin to visualize ipRGCs (*I* and *J*), and CART to visualize dsRGCs (*K* and *L*), in P25 wild-type and DKO retinas. (Magnification: *A* and *B*, 100×; *C–L*, 200×.) (*M*) Quantification of Tbr2$^+$ RGCs at different developmental stages. (*N* and *O*) Quantification of melanopsin$^+$ cells in *I–J* (*N*) and CART$^+$ cells in *K–L* (*O*). Student *t* test was applied to determine statistical significance. Error bars indicate ± SD. $n = 3$, $^*P \leq 0.05$, $^{**}P \leq 0.01$.

confirmed the changes of these genes in the DKO retina (Fig. 8 *E*, *G*, *I*, and *K*). Moreover, whereas the levels of *Pou6f2* and *Crabp1* were markedly reduced in all RGCs (Fig. 8 *E* and *G*), those of *Gfi1* and *Isl2* did not change in individual cells, but the numbers of cells expressing the two genes increased (Fig. 8 *I* and *K*). These results reinforced the idea that the onecut factors regulate the generation specific RGC subtypes. We also observed up-regulation of genes involved in rod development or function, including *Crx*, *Nrl*, *NeuroD*, *NeuroD4*, and *Pdc* (Fig. 8*C*). The up-regulation of *Crx* was further confirmed by in situ hybridization (Fig. 8 *L* and *M*). *Crx* is expressed in both rods and cones. Because no cones were produced in the DKO retina at E14.5, up-regulation of *Crx*, together with that of other rod genes, clearly indicates precocious rod differentiation in the DKO retina. Additionally, we also observed down-regulation of amacrine cell marker genes, such as *Th*, which is consistent with the overall reduction of amacrine cells in the DKO retina, but the mechanisms involved are unknown at the current time.

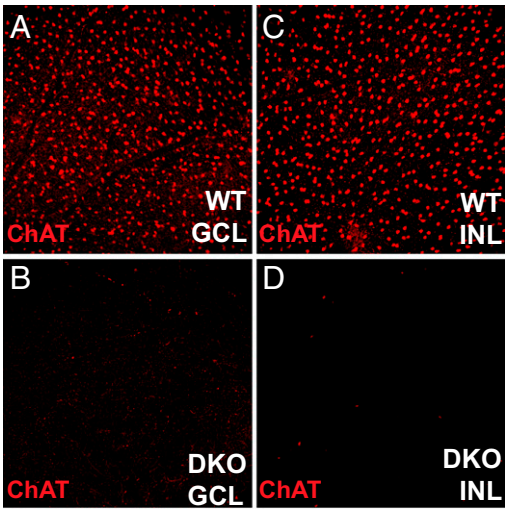

Fig. 7. SACs are diminished in DKO retinas. P25 whole retinas were stained for ChAT in WT and DKO retinas. (*A* and *B*) Confocal images taken at the focal level of the GCL. (*C* and *D*) Confocal images obtained at the focal level of the INL. (Magnification: 200×.)

Discussion

Redundancy of Oc1 and Oc2 in Retinal Development. In this study, we reveal that although knockout of *Oc1* or *Oc2* led to only partial loss of HCs, deletion of both transcription factor genes resulted in more profound retinal defects involving all of the early retinal cell types, including HCs, RGCs, cones, and SACs, indicating that Oc1 and Oc2 function redundantly in regulating these cell fates. This conclusion is further supported by the overlap of genes affected in the retinas of single-knockouts, and by the fact that although a larger number of genes demonstrated significant changes of expression in DKO retinas, most of these genes also showed the same direction of changes in the single-knockout retinas. The severity of retinal phenotypes in the three different mutants correlated well with the levels of expression of the two factors (15), and with the relative numbers of genes significantly affected in each mutant. These results suggest that Oc1 and Oc2 contribute quantitatively to the expression of downstream genes. Oc1 and Oc2 are coexpressed in many other tissues during development. For example, Oc1 and Oc2

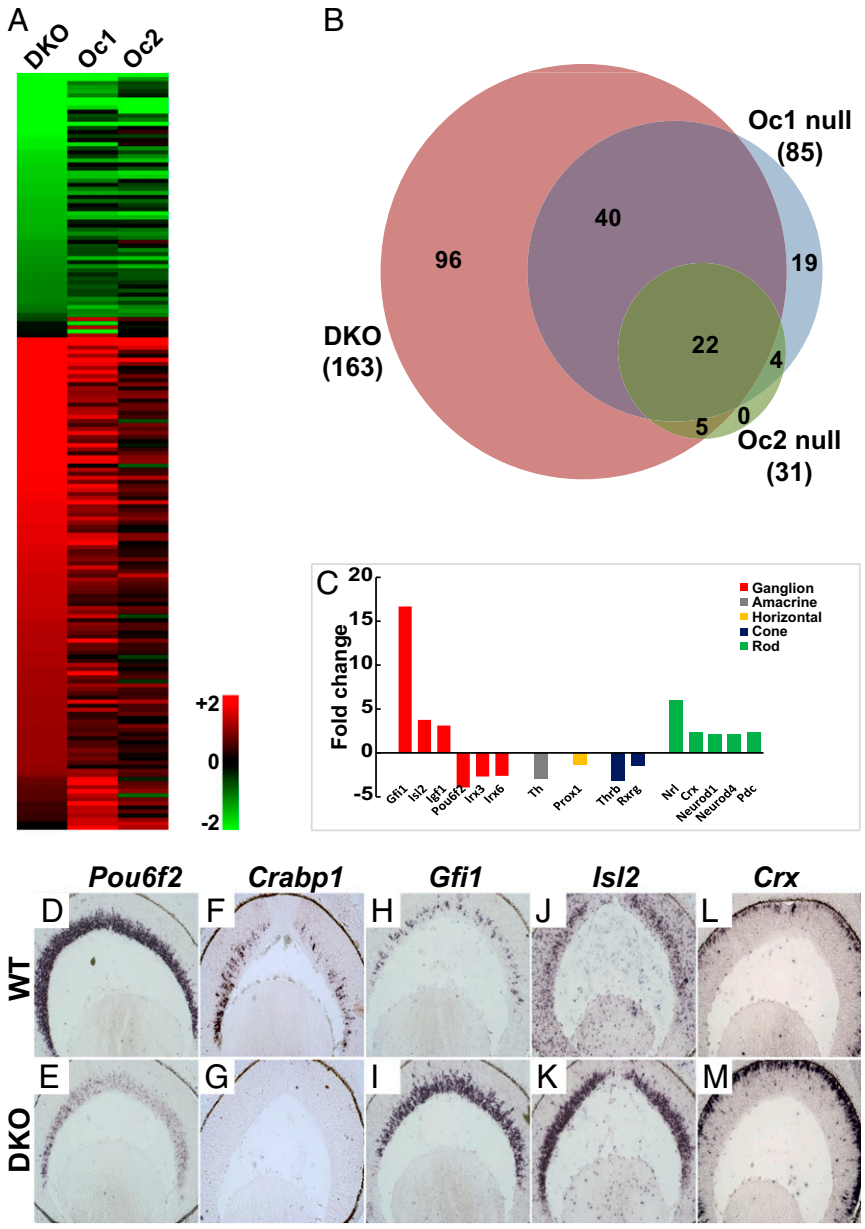

Fig. 8. RNA-Seq reveals alterations of gene expression in the DKO retina. (*A*) Heat map representation of genes differentially expressed by at least twofold in at least one of the three mutant retinas (DKO, *Oc1*-null, and *Oc2*-null) at E14.5. A color-coded $\log_2$ scale is shown at the bottom right of the heat map: red, up-regulation; green, down-regulation; black, no change. (*B*) A Venn diagram depicting the extensive overlap of genes altered in the three mutant retinas at E14.5. (*C*) Expression of some retinal cell-type–specific genes in E14.5 DKO retinas. Red, RGC-specific genes; gray, amacrin cell-specific gene; yellow, HC gene; blue, cone genes; green, rod genes. (*D–K*) In situ hybridization of four RGC genes, *Pou6f2* (*D* and *E*), *Crabp1* (*F* and *G*), *Gfi1* (*H* and *I*), and *Isl2* (*J* and *K*), and one photoreceptor gene *Crx* (*L* and *M*), confirms their changes in expression in the DKO retina at E14.5. (Magnification: *D–M*, 100×.)

also function redundantly in the developing motor neurons in the spinal cord (12). It is likely that the two factors regulate downstream genes in a similar fashion in other developing tissues.

Potential Mechanisms by Which Oc1 and Oc2 Function in Multiple Lineages. Our results indicate that Oc1 and Oc2 are required for all of the early retinal cell lineages. This finding is consistent with the timing of expression of these two factors; both are expressed in retinal progenitor cells at early—but not late—stages. Because specific sets of transcription factors are involved in individual cell types, an important question is whether a shared mechanism is involved to regulate all of the early cell fates. Our finding that the onecut factors serve as a common regulator for all of the early retinal fates indicates this may be the case. The absence of the onecut factors, at least in some cell lineages, leads to precocious production of late-born cell types. This finding indicates that the onecut factors contribute to maintaining the competence for the production of the early-born fates. Obviously, onecut factors are not the only factors involved in the RPC competence for the early retinal cell types, as some of the early cell types can still form in the DKO retina, albeit at much reduced levels. It is not clear what happens to the precursors of the early cell types in the absence of the onecut factors, as there is no corresponding increase in most late cell types, which may be a result of the decreased proliferation of progenitor cells at late stages. Although decreased cell proliferation unlikely contributes to the reduced production of the early cell types, it may lead to the reduced numbers of some of the late cell types.

Further study with genetic lineage tracing will clarify the fates of early-born precursors when the onecut factors are absent.

Conceivably, transition from the early to late competence would involve repression of the onecut factors. Several factors, including Lhx2 and a group of microRNAs (let-7, miR-125, and miR-9), have been identified to be involved in this transition (6, 7). Interestingly, all of the onecut genes are subject to repression by the microRNAs involved in the early-to-late transition (7), further supporting the important roles that the onecut factors play in generation of the early retinal cell types.

Roles of Oc1 and Oc2 in HC Development. *Oc1*- and *Oc2*-null retinas both exhibit a partial loss of HC genesis, but to different degrees. The less profound loss of HCs in *Oc2*-null retinas than in *Oc1*-null retinas is in agreement with the fact that Oc2 is expressed in a smaller cohort of HC precursors than Oc1 (15). Nevertheless, deletion of both *Oc1* and *Oc2* together leads to complete failure of HC genesis, confirming the redundancy of these two factors in the HC lineage. Two major regulators involved in the HC fate are FoxN4 and Ptf1a, with FoxN4 being upstream (29, 30). We recently showed that Oc1 functions together with Ptf1a at the same level in the regulatory hierarchy to promote the HC fate and inhibit the amacrine cell fate (14). Because Oc2 is closely related to Oc1, binds to the same DNA motif, and has a similar expression pattern, it is likely that Oc2 functions similarly in promoting the HC lineage. Interestingly, Otx2, a homeodomain transcription factor involved in photoreceptor fates, is also required for HC formation (31). It remains to be investigated how the onecut factors and Otx2 interact in the regulatory hierarchy of HC genesis.

Oc1 and Oc2 Are Involved in Cone Formation. The principle of photoreceptor development posits that a set of proliferating progenitors become generic photoreceptor precursors, which then differentiate into either cones or rods (5). Although there are no obvious cone defects in single-knockout retinas, DKO retinas exhibit a complete failure of cone genesis at E14.5, again demonstrating the redundancy of Oc1 and Oc2. At later stages, starting at around E17.5, some cones did develop in the DKO retina, but ultimately the numbers of cones were still reduced by ~30%. These results indicate that there are two distinct mechanisms for cone genesis: one that requires the onecut factors (operating in the early phase) and the other that is independent of the onecut factors (operating in the late phase). Additionally, we found that, in the DKO retinas, cones fail to diversify into the M-subtype, thus resulting in a concomitant overrepresentation of the S-subtype; this likely was caused by the down-regulation of Thrb, which is required for the differentiation of M-cones from the default S-cone pathway (18). Consistent with a previous study (17), we also observed precocious rod genesis, as indicated by the up-regulation of rod markers, such as Nrl and Crx, at E14.5. These results indicate that, at early stages, the onecut factors are required for cone genesis and for suppressing the rod fate.

Roles of Oc1 and Oc2 in RGC Development. Key regulators for RGC development include Atoh7 (also known as Math5), Pou4f2, and Isl1, with Atoh7 functioning upstream, and Pou4f2 and Isl1 downstream (32). Sox4 and Sox11 also seem to be involved in the early stages of RGC genesis, downstream of Atoh7 but independent of Pou4f2 (33). Oc1 and Oc2 are both expressed in RPCs and postmitotic RGCs, and thus appear to function at two levels: one during RGC genesis (at the same level as Atoh7) and the other after RGC genesis (downstream of Atoh7) to regulate RGC subtype specification (15). In postmitotic RGCs Oc1 and Oc2 reside in a distinct branch of the RGC regulatory network from Isl1 and Pou4f2, because they are not dependent on either Isl1 or Pou4f2 for expression (15). Currently we do not know the relationships between the onecut factors and the sox factors, although by RNA-Seq we did not see significant changes in Sox4 and Sox11 in the onecut mutants. Because there was only about 30% reduction in RGCs in *Oc1*/*Oc2* DKO retinas, not all RGCs require the onecut factors for genesis. As mentioned above, other unknown factors may regulate the production of the remaining RGCs. More significantly, our finding indicates that Oc1 and Oc2 are involved in the formation of distinct RGC subtypes, including ipRGCs, Crabp$^+$ RGCs, Isl2$^+$ RGCs, and Gfi1$^+$ RGCs. Interestingly, the onecut factors seem to promote certain subtypes but repress others. The generation of RGC subtypes has just begun to be studied (22) and the molecular markers for most RGC subtypes remain to be identified; therefore, we do not yet have a full picture of how Oc1 and Oc2 regulate RGC subtype formation. However, the many RGC genes identified in our RNA-Seq analysis, which are expressed in only subsets of RGCs, provide new opportunities for further studying the mechanisms underlying RGC subtype formation.

Materials and Methods

Mice. All procedures using mice conform to the US Public Health Service Policy on Humane Care and Use of Laboratory Animals and were approved by the Institutional Animal Care and Use Committees of the Roswell Park Cancer Institute and the University at Buffalo. All mice were maintained in a C57/BL6 × 129 genetic background. *Six3-Cre* transgenic and *Oc1^{flox}* mice, and their genotyping strategies, have been described previously (14). The *Oc2^{flox}* mouse line was generated as shown in Fig. S1*A*. Briefly, using recombineering (32), a targeting construct was generated by inserting a loxP site upstream of the transcription start site and a *loxP-FRT-Neo-FRT* cassette in the first intron of *Oc2* (Fig. S1*A*). This construct was then used to electroporate the G4 129xC57BL/6 F1 hybrid ES cells (32). After selection by G418 and ganciclovir, positive clones were identified by Southern blot hybridization with a 5′ external probe, in which the wild-type allele and correctly targeted allele yielded 13.1- and 4.0-kb fragments, respectively (Fig. S1 *A* and *B*). Two positive clones were then injected into C57/BL6 blastocysts to generate chimeric mice. High percentage chimeric males were crossed with wild-type C57BL/6 females for germ-line transmission, and the resulted progenies were genotyped for the presence of *loxP* and *Neo* by PCR. Positive progenies were then bred with the FLPeR mice (32) to delete the *Neo* cassette and generate *Oc2^{flox}* mice. All later genotyping were performed by PCR. The primers for genotyping *Oc2^{flox}* were: Oc2Fup 5′-CGT ACG ACA AGC TTA CAA GA-3′ and Oc2Fdn 5′-GGG TCG AAC GTT TCA GG TTT-3′.

Immunohistochemistry. Immunofluorescence staining of whole mount and cryo-sectioned retinas followed the protocols we have described previously (14, 15). Antibodies against Oc2, Prox1, Sox9, Isl1, vimentin, CAR, calbindin, Bassoon, Pou4f2, Lim1, ChAT, Tbr2 (Eomes), rhodopsin, Pax6, Pkcα, Nf160, and Chx10 were from multiple commercial sources, as reported by us before (14, 15, 32, 34). Other antibodies and their dilutions used in this study were: mouse anti-Pou4f1 (Millipore, MAB1585; 1:300), rabbit anti-CART (Phoenix Pharma, H00362; 1:1,000), rabbit anti-melanopsin (Advanced Targeting System, AB-N38; 1:1,000), rabbit anti-Rxrγ (Santa Cruz, SC555; 1:200), rabbit anti-blue (S) opsin (Millipore, AB5407; 1:400), and rabbit anti-red/green (M) opsin (Millipore, AB5405, 1:500). Secondary antibodies, propidium iodide, and anti-mouse IgG Fab fragments were used when necessary, as described elsewhere (14). Staining of cones by Alexa-488 conjugated PNA followed a previously published protocol (34).

EDU Labeling. A 10-mM solution of EDU (Invitrogen, C10337) in DMSO was injected into pregnant dams at the desired stages at 4 μL/g body weight. Embryos were harvested after 1 h, cryopreserved, and processed as for immunofluorescence staining. EDU was then detected using Click-iT Alex Fluor 488 imaging kit (Invitrogen, C10337) following the manufacturer's instructions.

TUNEL Assay. Apoptotic cells on retinal sections were detected using the Apop Tag Plus Fluorescein In Situ Apoptosis Detection Kit (Millipore, S7111) following the manufacturer's instructions and counted as previously described (14).

Confocal Imaging and Cell Counting. Confocal fluorescence images were collected using a Leica TCS SP2 confocal microscope as described previously (14). Image adjustment, when needed, was done identically for control and test specimens using Adobe Photoshop CS6. For cell counting on retinal sections, cells positive for a desired marker from arbitrary unit lengths in the central regions were counted. For whole-mount retinas, cells stained for

a desired marker in the corresponding regions from control and mutant retinas were counted. Counting was performed on a computer screen, either manually (for sections with sparse cells) or using ImageJ (for sections with many cells and for whole-mounts). In ImageJ (http://imagej.nih.gov/ij), particle analyzer was used to count cells after converting the images to 8 bit and adjusting the threshold. At least three ($n = 3$) sections or whole-mounts from different animals were counted, and a two-tailed, two-sample equal variance t test was performed; for statistical significance, $P < 0.05$ was considered significant and $P < 0.01$ highly significant.

Histology. H&E staining of retinal sections from paraffin-embedded eyes and light microscopy imaging was performed as reported previously (14). For Toluidine blue staining, microtome sections (0.5-μm thick) from plastic resin-embedded eyes were cut and placed onto precleaned glass microscope slides, which were then placed on a hot plate to let the section dry down. With the slide still on the hotplate, sections were covered with 1% Toluidine blue dissolved in 1% borax. After a desired time (10–90 s), the slides were rinsed with water and allowed to dry on the hot plate; after cooling in air, the slides were cover-slipped with Permount (EMS, 17986). Images were obtained with a Nikon Eclipse 80i microscope using a SPOT RT3 digital camera (Diagnostic Instruments).

Transmission Electron Microscopy. Mouse eyes and optic nerves were processed for resin embedment and transmission electron microscopy, as described previously (14).

RNA-Seq. After timed mating, E14.5 retinas from wild-type, *Oc1*-null, *Oc2*-null, and DKO embryos were collected in ice-cold PBS and treated overnight with RNAlater solution (Ambion, AM7020) at 4 °C, and stored at −80 °C. Total RNA was isolated/purified using the miRNeasy Mini Kit (Qiagen, 217004) along with on-column digestion of DNA with RNase-Free DNase Set (Qiagen, 79254) following the manufacturers' instructions. Three independent samples were prepared for each genotype. RNA quality was assessed by agarose gel electrophoresis, spectrophotometry, and a BioAnalyzer (Agilent, G2940CA). The samples were then used to generate sequencing libraries with TruSeq RNA Sample Prep Kit v2 kit (Illumina, RS-122-2001) and sequenced on an Illumina HiSeq. 2500 sequencer following the manufacturer's instructions. The sequence reads were mapped to the mouse genome using Bowtie (35), and differentially expressed genes were identified using Cufflinks2 (36). Genes with a false-discovery rate ≤ 0.05 were selected for further analysis. The sequence reads have all been deposited into the National Center for Biotechnology Information Sequence Read Archive (www.ncbi.nlm.nih.gov/sra, accession nos. SAMN02688949–SAMN02688960).

Quantitative RT-PCR. Two micrograms of total RNA were reverse-transcribed into first-strand cDNA using the SuperScriptII Reverse Transcriptase Kit (Invitrogen, 18064–014) and Oligo (dT)12–18 Primers (Invitrogen, 18418–012). Aliquots of cDNA equivalent of 0.1 μg total RNA from retinas of different genotypes were then used for real-time PCR, which was performed with the IQ SYBR Green Supermix (Bio-Rad, 170–18882) on an iCycler (Bio-Rad, 170–8720). PCR product specificities were ensured by melting curve analysis and 2% (wt/vol) agarose gel electrophoresis. The β-actin gene was used as control. qPCR conditions and primers used are listed in Table S1.

ACKNOWLEDGMENTS. We thank other members of our laboratory and members of Department of Ophthalmology and the Developmental Genomics Group for helpful discussions. RNA-Seq was performed by the Next-Generation Sequencing and Expression Analysis Core at the New York State Center of Excellence in Bioinformatics and Life Sciences, University at Buffalo. The $Oc2^{flox}$ allele was created with the help of the Gene Targeting and Transgenic Resource Core at the Roswell Park Cancer Institute. This project was supported by National Eye Institute Grants EY020545 (to X.M.) and EY007361 (to S.J.F.), the Whitehall Foundation (X.M.), the State University of New York/Research Foundation Research Collaboration Fund (to X.M. and S.J.F.), an unrestricted grant from Research to Prevent Blindness (to X.M. and S.J.F.), and resources and facilities provided by the Veterans Administration Western New York Healthcare System (S.J.F.).

1. Wässle H, Boycott BB (1991) Functional architecture of the mammalian retina. *Physiol Rev* 71(2):447–480.
2. Livesey FJ, Cepko CL (2001) Vertebrate neural cell-fate determination: Lessons from the retina. *Nat Rev Neurosci* 2(2):109–118.
3. Xiang M (2013) Intrinsic control of mammalian retinogenesis. *Cell Mol Life Sci* 70(14):2519–2532.
4. Young RW (1985) Cell differentiation in the retina of the mouse. *Anat Rec* 212(2):199–205.
5. Swaroop A, Kim D, Forrest D (2010) Transcriptional regulation of photoreceptor development and homeostasis in the mammalian retina. *Nat Rev Neurosci* 11(8):563–576.
6. Gordon PJ, et al. (2013) Lhx2 balances progenitor maintenance with neurogenic output and promotes competence state progression in the developing retina. *J Neurosci* 33(30):12197–12207.
7. La Torre A, Georgi S, Reh TA (2013) Conserved microRNA pathway regulates developmental timing of retinal neurogenesis. *Proc Natl Acad Sci USA* 110(26):E2362–E2370.
8. Lemaigre FP, et al. (1996) Hepatocyte nuclear factor 6, a transcription factor that contains a novel type of homeodomain and a single cut domain. *Proc Natl Acad Sci USA* 93(18):9460–9464.
9. Margagliotti S, et al. (2007) The Onecut transcription factors HNF-6/OC-1 and OC-2 regulate early liver expansion by controlling hepatoblast migration. *Dev Biol* 311(2):579–589.
10. Espana A, Clotman F (2012) Onecut transcription factors are required for the second phase of development of the A13 dopaminergic nucleus in the mouse. *J Comp Neurol* 520(7):1424–1441.
11. Espana A, Clotman F (2012) Onecut factors control development of the Locus Coeruleus and of the mesencephalic trigeminal nucleus. *Mol Cell Neurosci* 50(1):93–102.
12. Roy A, et al. (2012) Onecut transcription factors act upstream of Isl1 to regulate spinal motoneuron diversification. *Development* 139(17):3109–3119.
13. Iyaguchi D, Yao M, Watanabe N, Nishihira J, Tanaka I (2007) DNA recognition mechanism of the ONECUT homeodomain of transcription factor HNF-6. *Structure* 15(1):75–83.
14. Wu F, et al. (2013) Onecut1 is essential for horizontal cell genesis and retinal integrity. *J Neurosci* 33(32):13053–13065, 13065a.
15. Wu F, Sapkota D, Li R, Mu X (2012) Onecut 1 and Onecut 2 are potential regulators of mouse retinal development. *J Comp Neurol* 520(5):952–969.
16. Keeley PW, et al. (2013) Development and plasticity of outer retinal circuitry following genetic removal of horizontal cells. *J Neurosci* 33(45):17847–17862.
17. Emerson MM, Surzenko N, Goetz JJ, Trimarchi J, Cepko CL (2013) Otx2 and Onecut1 promote the fates of cone photoreceptors and horizontal cells and repress rod photoreceptors. *Dev Cell* 26(1):59–72.
18. Ng L, et al. (2001) A thyroid hormone receptor that is required for the development of green cone photoreceptors. *Nat Genet* 27(1):94–98.
19. Xiang M, et al. (1995) The Brn-3 family of POU-domain factors: Primary structure, binding specificity, and expression in subsets of retinal ganglion cells and somatosensory neurons. *J Neurosci* 15(7 Pt 1):4762–4785.
20. Mao CA, et al. (2008) Eomesodermin, a target gene of Pou4f2, is required for retinal ganglion cell and optic nerve development in the mouse. *Development* 135(2):271–280.
21. Sweeney NT, Tierney H, Feldheim DA (2014) Tbr2 is required to generate a neural circuit mediating the pupillary light reflex. *J Neurosci* 34(16):5447–5453.
22. De la Huerta I, Kim IJ, Voinescu PE, Sanes JR (2012) Direction-selective retinal ganglion cells arise from molecularly specified multipotential progenitors. *Proc Natl Acad Sci USA* 109(43):17663–17668.
23. Elshatory Y, Deng M, Xie X, Gan L (2007) Expression of the LIM-homeodomain protein Isl1 in the developing and mature mouse retina. *J Comp Neurol* 503(1):182–197.
24. Zhou H, Yoshioka T, Nathans J (1996) Retina-derived POU-domain factor-1: A complex POU-domain gene implicated in the development of retinal ganglion and amacrine cells. *J Neurosci* 16(7):2261–2274.
25. Wallis D, et al. (2003) The zinc finger transcription factor Gfi1, implicated in lymphomagenesis, is required for inner ear hair cell differentiation and survival. *Development* 130(1):221–232.
26. Triplett JW, et al. (2014) Dendritic and axonal targeting patterns of a genetically-specified class of retinal ganglion cells that participate in image-forming circuits. *Neural Dev* 9(1):2.
27. Brown A, et al. (2000) Topographic mapping from the retina to the midbrain is controlled by relative but not absolute levels of EphA receptor signaling. *Cell* 102(1):77–88.
28. McCaffrery P, Posch KC, Napoli JL, Gudas L, Dräger UC (1993) Changing patterns of the retinoic acid system in the developing retina. *Dev Biol* 158(2):390–399.
29. Fujitani Y, et al. (2006) Ptf1a determines horizontal and amacrine cell fates during mouse retinal development. *Development* 133(22):4439–4450.
30. Li S, et al. (2004) Foxn4 controls the genesis of amacrine and horizontal cells by retinal progenitors. *Neuron* 43(6):795–807.
31. Sato S, et al. (2007) Dkk3-Cre BAC transgenic mouse line: A tool for highly efficient gene deletion in retinal progenitor cells. *Genesis* 45(8):502–507.
32. Mu X, Fu X, Beremand PD, Thomas TL, Klein WH (2008) Gene regulation logic in retinal ganglion cell development: Isl1 defines a critical branch distinct from but overlapping with Pou4f2. *Proc Natl Acad Sci USA* 105(19):6942–6947.
33. Jiang Y, et al. (2013) Transcription factors SOX4 and SOX11 function redundantly to regulate the development of mouse retinal ganglion cells. *J Biol Chem* 288(25):18429–18438.
34. Mu X, et al. (2005) Ganglion cells are required for normal progenitor-cell proliferation but not cell-fate determination or patterning in the developing mouse retina. *Curr Biol* 15(6):525–530.
35. Langmead B, Trapnell C, Pop M, Salzberg SL (2009) Ultrafast and memory-efficient alignment of short DNA sequences to the human genome. *Genome Biol* 10(3):R25.
36. Trapnell C, et al. (2012) Differential gene and transcript expression analysis of RNA-seq experiments with TopHat and Cufflinks. *Nat Protoc* 7(3):562–578.